Polymer Chemistry

Highly conductive mechanically robust high Mw polyfluorene anion exchange membrane for alkaline fuel cell and water electrolysis application

Journal:	*Polymer Chemistry*
Manuscript ID	PY-ART-03-2020-000334.R1
Article Type:	Paper
Date Submitted by the Author:	27-Apr-2020
Complete List of Authors:	Miyanishi, Shoji; Tokyo Institute of Technology, Chemical Resources Laboratory Yamaguchi, Takeo; Tokyo Institute of Technology, Laboratory for Chemistry and Life Science

Journal Name

ARTICLE

Received 00th January 20xx,

Accepted 00th January 20xx

DOI: 10.1039/x0xx00000x

www.rsc.org/

Highly conductive mechanically robust high M_w polyfluorene anion exchange membrane for alkaline fuel cell and water electrolysis application

Shoji Miyanishi*[a,b] and Takeo Yamaguchi*[a,b]

New, high molecular weight poly-(fluorene-*alt*-tetrafluorophenylene) anion exchange membranes were synthesized by a Pd-catalyzed C–H activation method. The synthesized membranes exhibited high OH^- conductivity over 100 mS/cm, and membrane swelling could be suppressed by controlling the side chain length of the polymers. The membranes were flexible with high tensile strengh (25–42 MPa), which is comparable to Nafion 211 and likely because of their high molecular weight (M_w = 170–240 kDa). Conductivity and mechanical flexibility of the membranes did not vary significantly in 8 M NaOH at 80°C for 168 h. These membranes hold promise for both membrane and solid ionomer materials that can be used in alkaline fuel cells or alkaline water electrolysis devices.

Introduction

Fuel cells and water electrolysis cells have drawn growing interest for their potential to assist in the realization of a hydrogen-based clean-energy society. Hydrogen can be produced and stored by water electrolysis cells using renewable energy and converted to electricity using fuel cells without CO_2 emissions when necessary. Polymer electrolyte fuel cells (PEFCs) and water electrolysis cells that use proton exchange membranes are well-established and popular technologies. However, because these cells are operated in a highly corrosive acidic environment, only Pt-based metals can be used as effective electrode catalysts. Solid alkaline fuel cells and alkaline water electrolysis devices using anion exchange membranes (AEMs) are thus currently drawing attention as alternatives because cheaper non-noble metal-based electrode catalysts can be used in such devices [1–5]. Although a perfluorosulfonic acid membrane has already been developed as a highly durable membrane for use in proton exchange membrane fuel cells and water electrolysis cells, the development of a highly durable AEM remains critical for realizing the long-term operation of the cell.

Recent studies investigating the alkaline degradation mechanism of AEM have demonstrated that the structure of the membrane backbone is very important for obtaining a durable AEM. For example, typical poly (ether sulfone) or polyphenylene oxide AEMs decompose quickly due to cleavage of the ether linkages in their backbones [6]. In the case of benzyl alkyl ammonium-modified AEMs, cleavage of the ether linkages not only leads to polymer backbone degradation but also triggers degradation of the anion exchange group through the formation of unstable quinone methide structures [7,8]. For this reason, recently developed AEMs with ether-free backbones, such as polyphenylene [9-11] or polyphenylene alkylene [12–14], are promising candidates for use as highly durable and easily processable AEMs.

In addition to the aforementioned issue with respect to chemical durability, the mechanical stability of AEMs is also an important issue. During preparation and operation of fuel cells and water electrolysis cells, long-term mechanical pressure is applied to the membrane. This often leads to the formation of pinholes or mechanical fractures in the membrane. Even if a chemically stable membrane is used, cell performance will be completely lost before chemical degradation of the material occurs. Therefore, the development of an AEM with both high chemical stability and high mechanical strength is important for future application. In general polymeric materials, mechanical strength and flexibility of the membrane is improved by chain entanglement and this entanglement increases with molecular weight of the polymer.

Compared with typical polyarylene ether engineering plastic-based AEMs, the mechanical strength of ether-free aromatic AEMs is generally lower because polymer entanglement cannot easily occur

[a] *Laboratory for Chemistry and Life science, Institute of Innovative Research, Tokyo Institute of Technology, 4259, Nagatsuta, Midori-ku, Yokohama 226-8503, Japan*
[b] *Core Research for Evolutionary Science and Technology, Japan Science and Technology Agency (JST-CREST)*

Electronic Supplementary Information (ESI) available: [details of any supplementary information available should be included here]. See DOI: 10.1039/x0xx00000x

in their ether-free backbones [15]. To prepare mechanically strong membranes, the development of high molecular weight polymers is critical for this type of AEM.

However, typical polyphenylene-based materials often suffer from low solubility due to the strong π–π stacking interactions in their backbones. In addition, most of these polymers are synthesized using a metal-catalyzed coupling method, with one exception to this being the recently developed polyphenylene [9] or polyphenylene alkyne polymers [12]. Polymers with a high molecular weight >100 kDa are difficult to obtain using this method [16].

Recently, Wakioka et al. reported the creation of poly (fluorene-*alt*-tetrafluorophenylene) engineering plastic using a Pd-catalyzed C–H activation method. Remarkably, this polymer is both soluble and has an high molecular weight of >300 kDa [17]. Although it is not a polyelectrolyte, proper modification of its side chain structure might afford a high-performance AEM with high mechanical strength and high solubility, which is critically important for fuel cell and water electrolysis cell applications.

In this work, we report the synthesis and resulting properties of a high molecular weight poly (fluorene-*alt*-tetrafluorophenylene) AEM. The polymers designed herein have entirely aromatic backbones without ether linkages or benzylic C–H bonds, which act as decomposition sites for alkalines. Accordingly, we expect that the designed polymer is a high-performance AEM with both high chemical durability and high mechanical strength applicable to these devices.

Experiments

Synthesis

2,7-dibromo-9,9-bis(6-chlorohexyl)fluorene (1)

In a 500-mL two-necked flask, 150 g of KOH was dissolved into 300 ml of water. *n*-Bu_4NCl (556 mg) was then added, and the mixture was stirred under a nitrogen atmosphere. 2,7-dibromofluorene (4.86 g, 15 mmol) was then dissolved in 1,6-dichlorohexane (23.3g, 150 mmol) by heating. The resulting solution was transferred to the 500-mL two-necked flask via a syringe under nitrogen atmosphere. The mixture was then stirred at 90°C under nitrogen atmosphere until the color of the organic layer changed from orange to ultramarine (approximately 90 min). After cooling the solution, the organic layer was extracted, and dichloromethane was added. The organic layer was acidified with 1 M HCl aq. and then washed twice with water. The solvent was then removed by a rotary evaporator, and the 1,6-dichlorohexane in the residue was removed in a vacuum ($<10^{-1}$ mmHg) at 110°C. Chromatography of the residue (hexane:chloroform = 9:1) afforded 2,7-dibromo-9,9-bis(6-chlorohexyl)fluorene (1) (6.31 g)with a 75% yield.

^{1}H-NMR ($CDCl_3$, 400 MHz): δ 7.52 (2H, m), δ 7.45 (4H, m), δ 3.42 (4H, t), δ 1.92 (4H, t), δ 1.59 (4H, m), δ 1.20 (4H, m), δ 1.08 (4H, m), δ 0.59 (4H, m)

2,7-dibromo-9,9-bis(8-chlorooctyl)fluorene (2)

To synthesize 2,7-dibromo-9,9-bis(8-chlorooctyl)fluorene, a similar synthetic procedure to that used for 2,7-dibromo-9,9-bis(6-chlorohexyl)fluorene was applied. The 2,7-dibromo-9,9-bis(8-chlorooctyl)fluorene (2) was obtained from 2,7-dibromofluorene and 1,8-dichlorooctane with a 71% yield.

^{1}H-NMR ($CDCl_3$, 400 MHz): δ 7.53 (2H, d), δ 7.46 (4H, m), δ 3.48 (4H, t), δ 1.91 (4H, t), δ 1.69 (4H, m), δ 1.31 (4H, m), δ 1.12–1.06 (12H, m), δ 0.57 (4H, m)

2,7-dibromo-9,9-bis(10-chlodecyl)fluorene (3)

To synthesize 2,7-dibromo-9,9-bis(10-chlorooctyl)fluorene, a similar synthetic procedure to that used for 2,7-dibromo-9,9-bis(6-chlorohexyl)fluorene was applied, though a different elusion solvent (hexane) was used for column chromatography. 2,7-dibromo-9,9-bis(10-chlorodecyl)fluorene (3) was obtained from 2,7-dibromofluorene and 1,10-dichlorooctane with a 74% yield.

^{1}H-NMR ($CDCl_3$, 400 MHz): δ 7.52 (2H, m), δ 7.46 (4H, m), δ 3.51 (4H, t), δ 1.91 (4H, t), δ 1.73 (4H, m), δ 1.36 (4H, m), δ 1.20 (8H, m), δ 1.11–1.05 (12H, m), δ 0.58 (4H, m)

PFOTFPh-C_6-Cl

The first synthesized solution (1) (1.12 g, 2 mmol), pivalic acid (204 mg, 2 mmol), $CsCO_3$ (1.96 g, 6 mmol), 14 mg P(*o*-C_6H_4-$OMe)_3$, and 10.4 mg $Pd_2(dba)_3$-$CHCl_3$ were added to a two-necked 50-mL flask. Three milliliters of dry tetrahydrofuran (THF) was further added to the flask, and the reaction mixture was stirred under nitrogen atmosphere for 15 min. Tetrafluorophenylene (309 mg, 2.06 mmol) was dissolved in 1-mL dry THF and immediately added to the flask via a syringe. The mixture was stirred at 25°C for 30 min under a nitrogen atmosphere and then again for 24 h at 80°C. The reaction was then quenched with 1 M HCl solution and extracted using chloroform. The mixture, containing HCl solution and chloroform, was then stirred for 6 h at 40°C. The soluble part of the mixture was collected, and the organic layer was washed with water three times. The mixture was concentrated on a rotary evaporator, and the residue was reprecipitated in MeOH. The solid was collected by filtration and dried in a vacuum. PFOTFPh-C6-Cl (0.98 g) was afforded with an 89% yield.

^{1}H-NMR ($CDCl_3$, 400 MHz): δ 7.92 (2H, d), δ 7.56 (4H, m), δ 3.44 (4H, t), δ 2.07 (4H, t), δ 1.63 (4H, m), δ 1.27 (4H, m), δ 1.56 (4H, m), δ 0.69 (4H, m) ^{19}F-NMR ($CDCl_3$, 400 MHz): δ-144.1

PFOTFPh-C_8-Cl

To synthesize PFOTFPh-C_8-Cl, a procedure similar to that used for PFOTFPh-C_6-Cl was applied. PFOTFPh-C_8-Cl was obtained from Solution 2 (2 mmol) with a 56% yield.

^{1}H-NMR ($CDCl_3$, 400 MHz): δ 7.91 (2H, d), δ 7.56 (4H, m), δ 3.48 (4H, t), δ 2.05 (4H, t), δ 1.70 (4H, m), δ 1.32 (4H, m), δ 1.13 (4H, m), δ 0.78 (4H, m) ^{19}F-NMR ($CDCl_3$, 400MHz): δ-144.1

PFOTFPh-C_{10}-Cl

To synthesize PFOTFPh-C_{10}-Cl, a procedure similar to that used for PFOTFPh-C_6-Cl was applied. PFOTFPh-C_{10}-Cl was obtained from (2) (2 mmol) with an 82% yield.

^{1}H-NMR ($CDCl_3$, 400 MHz): δ 7.92 (2H, m), δ 7.57 (4H, m), δ 3.50 (4H, t), δ 2.06 (4H, t), δ 1.73 (4H, m), δ 1.37 (4H, m), δ 1.17 (20H, m), δ 0.78 (4H, m) ^{19}F-NMR ($CDCl_3$, 400MHz): δ-144.1

PFOTFPh-C_6-TMA

Eight-hundred milligrams of PFOTFPh-C_6-Cl was dissolved into 50-mL chlorobenzene by heating in a 100-mL closed vial, and the solution was filtered to remove the insoluble polymer fraction. Three milliliters of trimethylamine (TMA) in a 28% methanol solution was then added to the solution, and the mixture was stirred for 10 h at 105°C in the closed vial. The solution was cooled, and 20-mL dimethyl sulfoxide was added. The mixture was stirred for 6 h at 105°C and then cooled once more. Most of the chlorobenzene in the solution was removed on a rotary evaporator, and 20-mL dimethyl sulfoxide along with 3-mL trimethylamine in a 28% methanol solution was added to the solution. The mixture was stirred for 6 h and then cooled. The dimethyl sulfoxide in the solution was removed on a rotary evaporator, and water was added to afford the membrane. The membrane was then washed with hot water (80°C) three times and dried in a vacuum. PFOTFPh-C_6-TMA was afforded with a 92% yield.

^{1}H-NMR (CD_3OD, 400 MHz): δ 8.06 (2H, d), δ 7.67 (4H, m), δ 3.25 (4H, t), δ 3.08 (18H, s), δ 2.22 (4H, br), δ 1.67 (8H, m), δ 1.23 (4H, m), δ 0.80 (4H, br) ^{19}F-NMR (CD_3OD, 400 MHz): δ-146.0

PFOTFPh-C_8-TMA

To synthesize PFOTFPh-C_8-TMA, a procedure similar to that used for PFOTFPh-C_6-TMA was applied. PFOTFPh-C_8-TMA was obtained from PFOTFPh-C_8-Cl with a 93% yield.

^{1}H-NMR (CD_3OD, 400 MHz): δ 8.06 (2H, d), δ 7.67 (4H, m), δ 3.29 (4H, t), δ 3.09 (18H, s), δ 2.18 (4H, br), δ 1.71 (4H, m), δ 1.27 (8H, m), δ 1.16 (4H, m), δ 0.74 (4H, br) ^{19}F-NMR (CD_3OD, 400 MHz): δ-146.1

PFOTFPh-C_{10}-TMA

To synthesize PFOTFPh-C_{10}-TMA, a procedure similar to that used for PFOTFPh-C_6-TMA was applied. PFOTFPh-C_{10}-TMA was obtained from PFOTFPh-C_{10}-Cl with a 91% yield.

^{1}H-NMR (CD_3OD, 400 MHz): δ 8.06 (2H, m), δ 7.67 (4H, m), δ 3.29 (4H, t), δ 3.11 (18H, t), δ 2.16 (4H, m), δ 1.74 (4H, m), δ 1.32-1.14 (24H, m), δ 0.72 (4H, m) ^{19}F-NMR (CD_3OD, 400 MHz): δ-146.1

Measurement

Proton nuclear magnetic resonance (^{1}H-NMR) spectra were recorded on a Bruker Biospin Avance III system (400 MHz). Gel permeation chromatography (GPC) was performed on a high-performance liquid chromatography L-7100 system (Hitachi Corp.) equipped with a UV detector and Asahipak GF-7MHQ columns (×2) at 40°C using $CHCl_3$ as an eluent. The molecular weights were calculated against polystyrene standards. Water adsorption of the membrane was recorded on a MSB-AD-V-FC system (BEL Japan Inc.). The membrane was pretreated in a vacuum at 70°C for 90 min. Carbon, hydrogen, and nitrogen content in the membranes (20–30 μm in thickness) were analyzed using Micro Corder JM-10 (Japan Science Lab Co. Ltd.). Halide content in the membranes was analyzed using HSU-20 0 (Japan Science Lab Co. Ltd.).

In-plane anion (Cl^- and OH^-) conductivity was measured using the AC impedance method with a Solartron 1260 Impedance/Gain-Phase Analyzer in a frequency range of 1–10^6 Hz and with a signal amplitude range of 10–100 mV. The measurement conditions were controlled by a SH-221 Bench-top Type Temperature and Humidity Chamber (Espec Corp., Japan). For OH^- conductivity measurements, the polymer membranes (Cl^-) were soaked in 1 M NaOH aq. for 24 h to exchange Cl^- anions for OH^- anions and subsequently soaked in pure water for 2 h to remove residual NaOH in the glove box. The membrane was then set in a closed chamber, and resistance was measured in water under nitrogen atmosphere.

Tensile strength test

A tensile strength test was carried out using the INSTRON Universal Testing System 5985. The samples were cut into dumbbell shapes for the test (JIS-K6251-7). Stress–strain curves were obtained in air at 23°C and a stretching rate of 100 mm min^{-1} (chuck distance = 20 mm).

Alkaline stability test

In advance of the alkaline stability test, the Cl^- anions in the membrane were exchanged for OH^- by soaking in 1 M NaOH aq. for 24 h. The conductivity of the resulting membrane was measured at 80°C in air with RH = 95%. The membrane was then soaked in 8 M NaOH aq. in a high-density polyethylene closed vial. The temperature of the vial was set to 80°C via a FS-30W Bench-top Type Temperature Chamber (TGK, corp. Japan). After 168 h, the membrane was washed and soaked in pure water. The conductivity of the resulting membrane was measured at 80°C in air with RH = 95% and compared with the initial value.

Result and Discussions

The procedure for synthesis of trimethylammonium (TMA)-modified poly (fluorene-*alt*-tetrafluorophenylene) (PFOTFPh-C_x-TMA) is shown in Scheme 1. The monomers were synthesized in a single step from 2,7-dibromofluorene and dichloroalkane. The polymerization was conducted according to the method described in [17]. During optimization of the polymerization condition, we discovered two important issues for obtaining well-defined polymers. First, the end group of the side chain in the monomer must be a chloride group rather than a bromide or iodide group. This is because bromide and iodide will react with pivalic acid salt to afford pivalic ester during polymerization. Second, as far as we have investigated, the best reaction temperature for polymerization is 80°C. Polymerization at 70°C produced only low molecular weight oligomers, while polymerization at 95°C afforded a high insoluble polymer fraction. The reaction at 80°C afforded polymer without decreasing its molecular weight and also suppressed the formation of the insoluble polymer fraction. The origin of the insoluble polymer fraction may be the extremely high molecular weight polymer fraction or cross-linked polymers created by an unknown side reaction.

Figure 1 shows ^{1}H-NMR and fluorine-19 nuclear magnetic resonance (^{19}F-NMR) spectra of PFOTFPh-C_6-Cl after polymerization. The ^{1}H-NMR spectra reveal a peak at 3.42 ppm derived from the –CH_2-Cl group. The integration ratio between this peak and the aromatic protons at 7–8 ppm is almost consistent with the theoretical value, indicating that the alkyl chloride group of the side chain is stable under polymerization conditions. ^{19}F-NMR shows a high and sharp peak at –144.2 ppm and very minor peaks at –139.1 and –143.7 ppm derived from the end group of the polymer. Similar conclusions were obtained for both PFOTFPh-C_8-Cl and PFOTFPh-C_{10}-Cl (Supporting Information S2). These NMR spectra indicate the formation of a polymer with a well-defined structure although a partly insoluble polymer could also have been produced.

Table 1 summarizes the molecular weights of the precursor polymers. The number average molecular weights (M_n) and weight average molecular weights (M_w) were M_n = 30 kDa and M_w = 178 kDa for PFOTFPh-C_6-TMA, M_n = 23 kDa and M_w = 170 kDa for PFOTFPh-C_8-TMA, and M_n = 37 kDa and M_w = 240 kDa for PFOTFPh-C_{10}-TMA. It should be noted that the molecular weights of the polymerizations could in reality be larger than these values since only the molecular weight of the soluble polymer could be measured.

Table 1. Molecular weight of PFOTFPh-C_x-Cl polymers

Polymer	M_n	M_w	PDI
PFOTFPh-C_6-Cl	30000	178000	5.9
PFOTFPh-C_8-Cl	23000	170000	7.4
PFOTFPh-C_{10}-Cl	36000	240000	6.5

Although the polydispersity value of typical step growth polymerization is approximately two, relatively large polydispersity (approximately 5–7) was reproducibly obtained in these polymerizations. This is because the polymerization had to be conducted at a temperature higher than the boiling point of the reaction solvent (>80°C) and therefore tended to proceed inhomogeneously. In addition, keeping the molar ratio of the two monomers at 80°C was difficult due to the highly volatile nature of the tetrafluorophenylene. Thus, the number average molecular weight of the polymer may have been suppressed given the current polymerization conditions. The resulting precursor polymer (PFOTFPh-C_x-Cl) could be dissolved in chloroform, toluene, and chlorobenzene (except for its completely insoluble fraction).

The chloride group of the PFOTFPh-C_x-Cl polymer was converted to trimethylammonium chloride using trimethylamine. After the reaction, the peak derived from the trimethylammonium group ($((CH_3)_3$-N^+-) was observed at 3.1 ppm. By comparing the peak integration at 3.1 ppm and the peak derived from the aromatic backbone at 7.5–8.5 ppm, it was concluded that almost all of the chloride groups were quaternized.

All PFOTFPh-C_x-TMA (x = 6, 8, 10) polymers were soluble in dimethyl sulfoxide, methanol, and typical alcoholic/water mixture solvents used for membrane electrode assembly (MEA) preparation. Details on the solubility of these polymers are summarized in Supporting Information (S3). The PFOTFPh-C_x-TMA(Cl^-) membranes were prepared by drop-casting of the polymer solution in dimethyl sulfoxide (DMSO) at 110°C. The prepared membranes were washed with hot water (60°C) three times to remove residual DMSO.

Figure 2 shows the appearance of the PFOTFPh-C_x-TMA(Cl^-) membranes. All of the membranes were transparent and flexible. Figure 3 shows the typical stress–strain curves of the PFOTFPh-C_x-TMA membranes. The PFOTFPh-C_6-TMA(Cl^-), PFOTFPh-C_8-TMA(Cl^-), and PFOTFPh-C_{10}-TMA(Cl^-) membranes demonstrated 42.3, 40.9, and 33.6 MPa tensile strengths, respectively. Also, the PFOTFPh-C_6-TMA(OH^-), PFOTFPh-C_8-TMA(OH^-), and PFOTFPh-C_{10}-TMA(OH^-) membranes demonstrated 26.8, 28.5, and 40.9 MPa tensile strengths, respectively (Figure 3b). These values are comparable to those of typical commercially available polyelectrolyte membranes, such as Nafion 117 and Nafion 212 (15-40 MPa)[18,19]. Thus, the PFOTFPh-C_x-TMA(Cl^-) membranes were mechanically strong enough for handling despite their highly rigid all-aromatic backbones.

Table 2 summarizes the ion exchange capacity (IEC), water uptake, and dimensional change of the membranes. All the membranes demonstrated low water uptake and high dimensional stability at 25°C. However, differences in water uptake and dimensional change became large at 80°C. This is probably because swelling of the polymers was suppressed or was kinetically very slow at room temperature due to the highly rigid backbones and intermolecular

π–π interactions. However, water was easily diffused in the membranes at 80°C, causing swelling of the polymers.

Table 2. Swelling of the membranes

AEM	IEC (meq)	Water uptake (%)[b]		Dimensional change (%)[b]	
	NMR	25 °C	80 °C	25 °C	80 °C
PFOTFPh-C_6-TMA (Cl-)	3.0	39	81	28	64
PFOTFPh-C_6-TMA (OH-)	3.2[a]	41	122	30	97
PFOTFPh-C_8-TMA (Cl-)	2.8	28	51	5.2	23
PFOTFPh-C_8-TMA (OH-)	2.9[a]	40	74	18	39
PFOTFPh-C_{10}-TMA (Cl-)	2.6	18	45	2.7	18
PFOTFPh-C_{10}-TMA (OH-)	2.7[a]	34	67	10	33
PES-TMA (OH^-)	2.9	593	-----[c]	364	-----[c]
PPO-TMA (OH^-)	3.0	243	-----[c]	221	-----[c]

[a] complete ion exchange from Cl^- to OH^- is assumed. [b] in water [c] membrane was broken

Although the water uptake and dimensional change of PFOTFPh-C_6-TMA were large at 80°C, these values were still lower than those of TMA-modified PES (IEC = 2.9) and PPO AEMs (IEC = 3.0) with similar IECs [20,21]. It should also be emphasized that the low molecular weight PFOTFPh-C_6-TMA (M_n = 3400, M_w = 6500) membrane had broken into pieces after being soaked into water and ultimately dissolved. Therefore, a high molecular weight fraction is critically important for obtaining mechanically strong membranes with low levels of swelling.

Figure 4 shows the water uptake and conductivity of the polymers under vapor conditions. Typical Nyquist Plots of the conductivity measurement are shown in Supporting Information (Figure S4). The PFOTFPh-C_6-TMA(Cl^-), PFOTFPh-C_8-TMA(Cl^-), and PFOTFPh-C_{10}-TMA(Cl^-) polymers demonstrated 133, 85, and 52 mS/cm conductivities, respectively, under RH = 95% at 80°C (Figure 4b). Arrehnius plot of the conductivity is shown in Figure 5. Their activation energies for conductivity were 20.3, 19.2, and 18.9 kJ/mol, respectively. Further, all of the PFOTFPh-C_x-TMA(Cl^-) membranes demonstrated a conductivity greater than 10^{-2} S/cm, even under low humidity RH = 60% at 80°C (Figure. 4b).

The humidity dependence of membrane conductivity was decreased when the alkyl chain length of the polymer side chain was increased [22]. Similar behavior was also observed in the proton exchange membranes. The chloride ions in the membranes were exchanged to hydroxide ions by soaking in 1M NaOH for 24h at 25 °C. Elemental analysis of PFOTFPh-C_{10}-TMA membrane with lowest water uptake was conducted to evaluate ion exchange. No chloride was detected after ion exchange in the PFOTFPh-C_{10}-TMA membrane (OH^-_{air}) while the chloride content of PFOTFPh-C_{10}-TMA membrane (Cl^-) is almost consistent to theoretical value (Table S3). This result confirms that most of chloride ions in the membranes were exchanged to OH^- ion.

The OH^- conductivity of the membranes was measured in water to diminish the possible effects of the carbon dioxide in the air. The measurement setup is shown in Supporting Information (Figure S5)

The PFOTFPh-C_6-TMA(OH^-), PFOTFPh-C_8-TMA(OH^-), and PFOTFPh-C_{10}-TMA(OH^-) membranes demonstrated 90.2, 68.3, and 58.7 mS/cm conductivities at 40°C, respectively, and 156, 117, and 101 mS/cm conductivities at 70°C, respectively. The activation energies for conductivity were 15.7, 14.7, and 17.3 kJ/mol, respectively (Figure 5). The activation energy of hydroxide conductivity was lower than that of chloride conductivity in all the membranes. This is because hydroxide ions can be conducted by both the vehicle and the Grotthuss mechanisms, while chloride can only be conducted by the vehicle mechanism [23]. These results indicate that the PFOTFPh-C_x-TMA membranes have a sufficiently high ion conduction behavior for application to alkaline fuel and water electrolysis cells.

Although the PFOTFPh-C_6-TMA membrane demonstrated very high ion conductivity over 0.1 S/cm, the dimensional change of the membrane at 80°C was also large, as shown in Table 2. Therefore, the PFOTFPh-C_8-TMA and PFOTFPh-C_{10}-TMA membranes are more suitable for real fuel cell or water electrolysis applications, as both high dimensional stability (<40%) and high OH^- conductivity (>0.1 S/cm) were maintained in these polymers.

Finally, the alkaline stability of the PFOTFPh-C_6-TMA membrane was investigated by soaking in 8 M NaOH aq. at 80°C for 168 h. Figure 6a shows the membrane appearance before and after the stability test. It was found that the membrane maintained its flexibility after the soaking. In contrast, typical PES AEMs were found to break into pieces after even 8 h soaking in 8 M NaOH aq. at 80°C [24]. This result indicates that PFOTFPh-C_6-TMA polymer is resistant to backbone scission, which is probably due to the fact that its backbone composed solely of aryl–aryl linkages. However, most of the polymer became insoluble after 24 h soaking in any solvent, thus making ^{1}H-NMR analysis difficult. This indicates that some cross-linking reaction took place in the polymer during the stability test. In addition, some color change was observed in the membrane after the alkaline stability test. Similar color changes and cross-linking behaviors were also observed in the PFOTFPh-C_8-TMA and PFOTFPh-C_{10}-TMA membranes.

Figure 6b shows the OH^- conductivity change of the PFTFPh-C_6-TMA membrane. The conductivity of the membrane was found to

decrease slightly after 168 h (86.2%). The stability of the membrane conductivity was much higher than that of benzyl trimethyl ammonium-modified polyarylene ether membranes. This claim is also supported by reports that have demonstrated high alkaline stability in compounds with small molecular weights [25] and in fluorene polymers with hexyl trimethylammonium groups [26]. The small decrease in conductivity was due to either a decrease in water uptake by polymer cross-linking or a gradual degradation of the anion exchange group.

We proposed a cross-linking mechanism for the PFTFPh-C_6-TMA membrane, as shown in Scheme 2. According to this proposal, one of the fluoride groups in the polymer backbone is substituted by a hydroxyl group via SN_2 reaction [8], which affords a phenoxide group in the alkaline solution. This group further attacks another fluoride group at the backbone to produce an ether linkage and cross-link the polymer. The color change of the membrane after the stability test may have been due to the changes in the conjugation length and absorption spectra of the polymer.

To clarify the degradation behavior of the PFTFPh-C_x-TMA membrane, a similar alkaline stability test was conducted using a low molecular weight model compound. The degradation product was analyzed by NMR and electrospray ionization time-of-flight mass spectrometry (ESI-TOF-MS). In the NMR analysis, no detectable degradation product was observed after 3 h in 8 M NaOH aq. at 80°C. After 200 h, however, NMR spectra of the degradation product broadened, and the peak pattern changed (Figure. S6). In the ^{1}H-NMR spectra, it was found that the peak integration at 3.1 ppm derived from the trimethylammonium group did not change significantly compared with the aromatic region at 7–8 ppm. However, the ^{19}F-NMR spectra of the model compound changed from having one peak to four (Figure. S6). These results also indicate that the backbone of the compound suffered from some chemical change, even though the anion exchange group remained stable.

ESI-TOF-MS of the degradation product after 200 h detected a compound in which one of the fluoride groups in the backbone had been substituted by a hydroxide group (Figure S7). It can thus be concluded that nucleophilic substitution of fluoride to hydroxyl occurred in this model compound.

It should be noted that the dimmer cross-linked by an ether linkage was not detected in the ESI-TOF-MS spectra (Scheme 2). However, formation of ether linkage between hexafluorophenylene and its potassium salt in dimethyl formamide has been reported [27].

We hypothesize that the phenoxide group formed by SN_2 reaction was not able to easily attack other fluoride groups in the model compound because the compound was surrounded mostly by water and OH^- anions. In contrast, the produced phenoxide could easily attack other fluoride groups in the membrane because the number of water molecules and OH^- anions in the membrane was limited and the phenoxide and fluoride groups were very close to one another. Therefore, one possible cross-linking reaction mechanism of the FTFPh-C_6-TMA membrane is defluorination and successive ether formation in the backbone. Park et al. reported a possible cross-linking mechanism between the hydroxyl group and contaminated alkyl bromide group in the sidechain [28]. However, our proposed cross-linking mechanism is more plausible in this case as contamination of alkyl chloride in the membrane is unlikely under our quaternization condition and alkyl chloride is much less reactive than alkyl bromide towards ether formation.

Although cross-linking reactions took place, the membrane maintained a high mechanical strength and high ionic conductivity. It can be concluded that one of the membrane's important properties is its stability in 8 M NaOH at 80°C.

Altogether, these results indicate that high molecular weight PFTFPh-C_x-TMA polymers have high conductivity and high alkaline durability. This material is promising for both membranes and ionomers of alkaline fuel cells and alkaline water electrolysis cells.

Conclusions

In this study, a novel ether-free all-aromatic AEM membrane was synthesized. The obtained membrane demonstrated high mechanical strength and flexibility owing to its high molecular weight. The membrane also demonstrated both high conductivity (>0.1 S/cm) and high dimensional stability (<40% at 80 ^{o}C) due to its alkyl side chain length and ion exchange capacity. Furthermore, the membrane maintained a high conductivity and mechanical flexibility after soaking in 8 M NaOH aq. at 80°C, indicating the high alkaline durability of the material. The membrane material shows suitable solubilities although it is not swell much in hot water (80°C).

The polymer developed in this work is a promising material for both membrane and ionomer applications in alkaline fuel and water electrolysis cells.

Acknowledgments

We thank Nissan ARC Corp. and Analytical Support Center at Tokyo Institute of Technology for tensile stress testing measurements and elemental analysis, respectively. This work is financially supported by Core Research for Evolutionary Science and Technology in Japan Science and Technology (JPMJCR1543).

Conflicts of interest

There are no conflicts to declare

Notes and references

1. Varcoe, J. R.; Slade, R. C. T. *Fuel cells* 2005, *5*, 187-200.
2. Hickner, M. A.; Herring, A. M.; Coughlin, E. B. *J. Polym. Sci. Part B: Polym. Phys.* 2013, *51*, 1727-1735.
3. S. Gottesfeld, D. R. Dekel, M. Page, C. Bae, Y. Yan, P. Zelenay, Y. S. Kim, *J. Power Sources*, 2018, 375, 170-184

4. K. F.L. Hagesteijn, S, Jiang, B.P. Ladewig, *J. Mater. Sci.* 2018, 53, 11131-11150
5. I. Vincent, D. Bessarabov, *Renew. Sust. Energy Rev.* 2018, 81, 1690-1704
6. Arges, C. G.; Ramani, V. *Proc. Nat. Acad. Sci.* 2013*, 110*, 2490-2495.
7. S. Miyanishi and T. Yamaguchi, *Phys. Chem. Chem. Phys.* 2016*, 18***,** 12009-12023
8. S. Miyanishi and T. Yamaguchi, *New J. Chem.* 2017, *41*, 8036.
9. Hibbs, M. R.; Fujimoto, C. H.; Comelius, C. J. *Macromolecules* 2009, *42*, 8316-8321.
10. Hibbs, M. R. *J. Polym. Sci., Part B: Polym. Phys.* 2013, 51, 1736–1742
11. H. P. R. Graha, S. Ando, S. Miyanishi and T. Yamaguchi *Chem. Commun.*, 2018, 54, 10820-10823
12. Lee, W. H.; Kim, Y. S., Bae, C. *ACS Macro Lett.* 2015, *4*, 814-818.
13. J. S. Olsson, T. H. Pham,P. Jannasch, *Adv. Funct. Mater.* 28, 1702758
14. S. Maurya**,** S. Noh**,** I. Matanovic**,** E. J. Park**,** C. N. Villarrubia**,** U. Martinez**,** J. Han**,** C. Bae and Y. S. Kim *Energy Environ. Sci.*, 2018, 11**,** 3283-3291
15. E. J Park, Y.S Kim, *J. Mater. Chem. A*, 2018, **6**, 15456-15477
16. S. Miyanishi and T. Yamaguchi, *J. Mater. Chem. A*, 2019, 7, 2219–2224
17. M. Wakioka,Y. Kitano,F. Ozawa, *Macromolecules* 2013, 46, 370-374
18. J. Lin, P.-H. Wu, R. Wycisk and P. N. Pintauro, *ECS transaction* 2008, 16, 1195-1204
19. X. Xu**,** L. Li**,** H. Wang**,** X. Li and X. Zhuang, *RSC Adv.*, 2015, 5**,** 4934-4940
20. S. S. He, A. S. Trickler and C. W. Frank, *ChemSusChem* 2015, 8, 1472-1483
21. N. Li, Y. Leng, M.A. Hickner, C.-Y. Wang *J. Am. Chem. Soc.* 2013, 135, 10124-10133
22. C. Jin, X.Zhu, S. Zhang, S. Li, *Polymer*, 2018, 149, 269-277
23. D. Dong, W. Zhang, A.C.T. van Duin and D. Bedrov. *J. Phys. Chem. Lett.* 2018, 9, 825-829
24. Chen, D.; Hickner, M. *ACS Appl. Mater. Interfaces* 2012, *4*, 5775–5781.
25. Mohanty, A. D.; C. Bae. C *J. Mater. Chem. A 2014,* 2, 17314-17320.
26. W.-H. Lee, A. D. Mohanty, C. Bae, *ACS Macro Lett.* 2015, 4, 453-457
27. L. A. Wall, W. J. Pummer, J. E. Fearn and J. M. Antonucci, *Res. Natl. Bur. Stand. A Phys. Chem.* 1963, 67A, 481-497
28. E. J. Park, S. Maurya, M. R. Hibbs, C. H. Fujimoto, K.-D. Kreuer, *Y. S. Kim, Macromolecules,* 2019, 52, 5419-5428

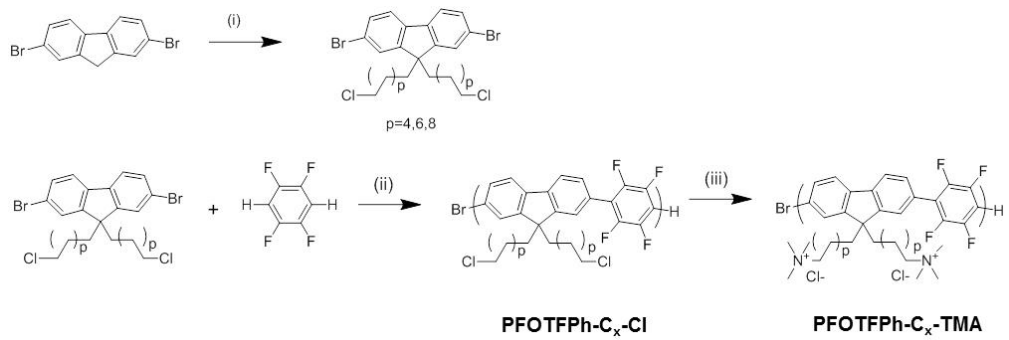

Scheme 1. Synthesis of PFOTFPh-Cx-TMA (x = 6, 8, 10)[a] [a]Reagents and conditions: (i) Cl-$(CH_2)_n$-Cl (n = 6, 8, or 10), n-Bu_4NCl, NaOH aq. 90°C (ii) $Pd_2(dba)_3$-$CHCl_3$, P(o-C_6H_4-OMe)$_3$, Cs_2CO_3, pivalic acid, dry THF, 80°C (iii) Trimethylamine, C_6H_5Cl-DMSO, 100°C

212x73mm (120 x 120 DPI)

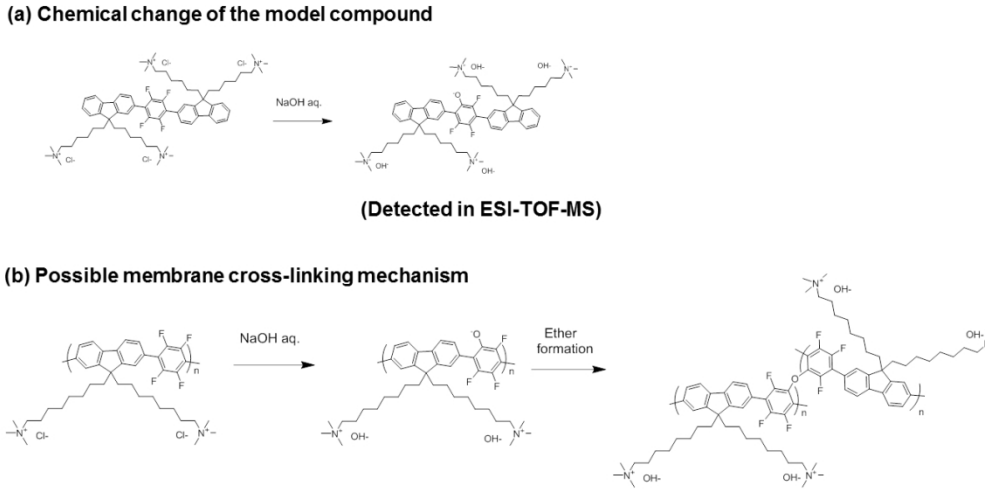

Scheme 2. (a) Alkaline degradation behavior of the low molecular weight model compound and (b) possible cross-linking mechanism of the membrane

355x266mm (96 x 96 DPI)

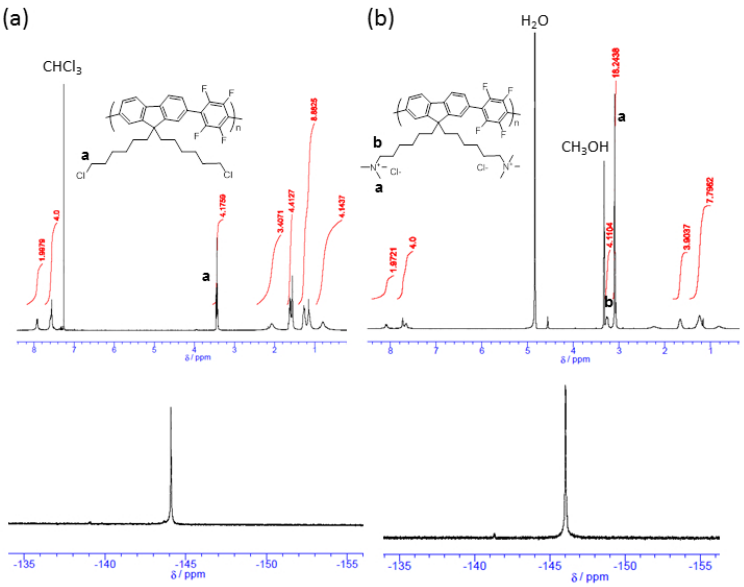

Figure 1. ^{1}H-NMR spectra and ^{19}F-NMR spectra of (a) PFOTFPh-C_6-Cl in $CDCl_3$ and (b) PFOTFPh-C_6-TMA in CD_3OD

254x190mm (96 x 96 DPI)

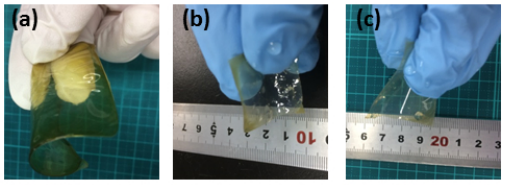

Figure 2. Appearance of the membranes (a) PFOTFPh-C_6-TMA (b) PFOTFPh-C_8-TMA (c) PFOTFPh-C_{10}-TMA

254x190mm (96 x 96 DPI)

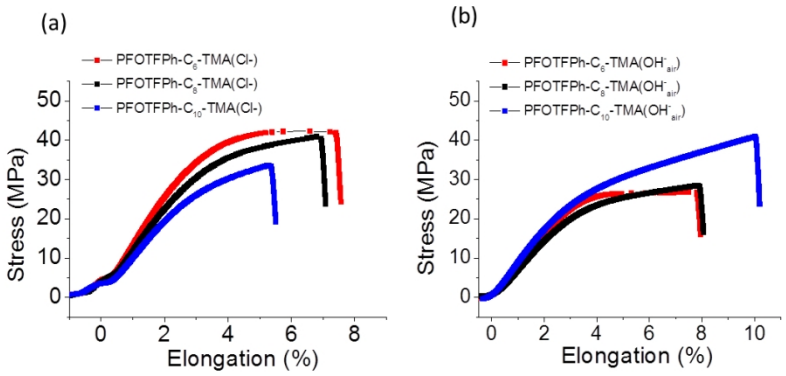

Figure 3. Typical stress-strain curve of (a) PFOTFPh-C_x-TMA(Cl^-) and (b) PFOTFPh-C_x-TMA(OH^-_{air}) membranes

355x266mm (96 x 96 DPI)

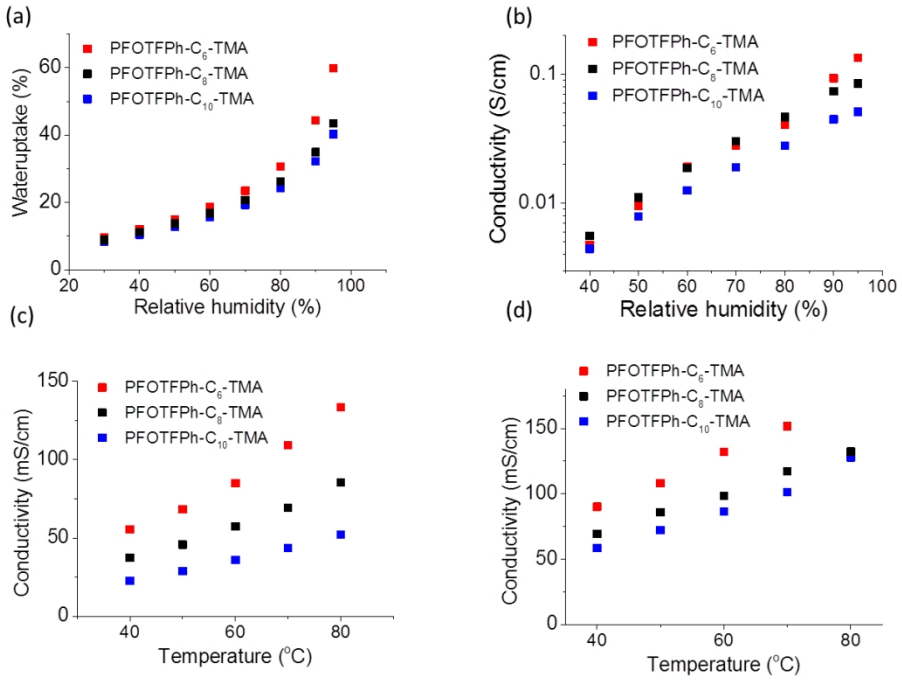

Figure 4. (a) Water uptake at 80°C as a function of humidity. (b) Chloride ion conductivity at 80°C as a function of humidity. (c) Chloride ion conductivity at RH = 95% as a function of temperature. (d) Hydroxide ion conductivity in water as a function of temperature of the PFOTFPh-C_x-TMA membranes[a]. [a] The data of PFOTFPh-C_6-TMA (OH^-) at 80 ^oC is not shown due to significant swelling in hot water

355x266mm (96 x 96 DPI)

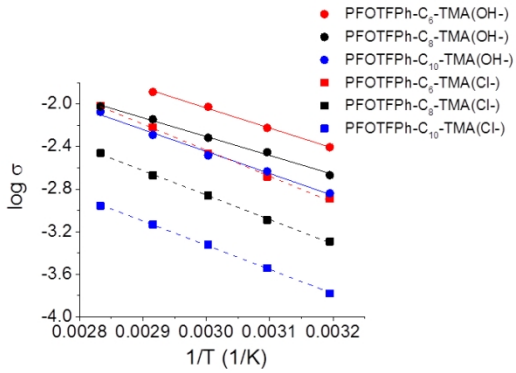

Figure 5. Arrhenius plot of the ionic conductivity

355x266mm (96 x 96 DPI)

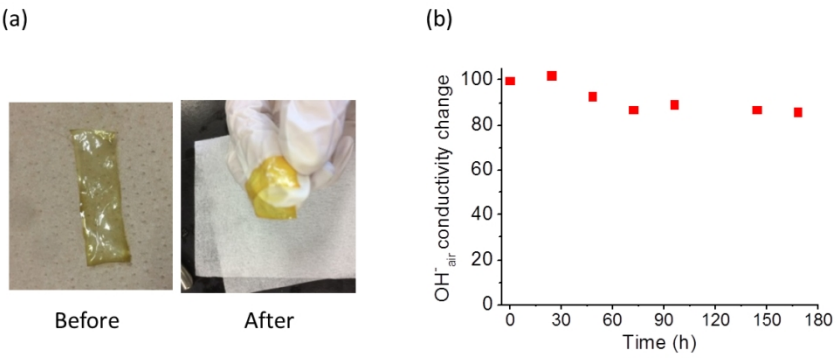

Figure 6. (a) Appearance and (b) OH^-_{air} conductivity changes of the PFOTFPh-C_6-TMA membrane before and after soaking in 8 M NaOH aq. for 168 h at 80°C.

355x266mm (96 x 96 DPI)

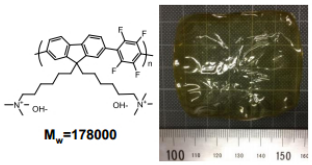

254x190mm (96 x 96 DPI)